SP 42-36

Moment Transfer To Columns In Slabs With Shearhead Reinforcement

By
N. W. Hawkins and W. G. Corley

Synopsis: The purpose of this investigation was to determine the effectiveness of shearhead reinforcement to increase the strength of slabs at their connection to edge columns. The 1971 ACI Building Code (ACI 318-71) permits the use of such shearheads only at interior column locations.

Results of tests on 14 slab-column specimens containing shearhead reinforcement and simulating conditions at an edge column in a flat plate structure are described. All specimens were made with lightweight aggregate concrete and Grade 60 high-strength reinforcement. The principal variables were the length and strength of the shearhead arms.

Two design methods for shearheads subjected to unbalanced moments at edge columns are presented. Modifications of the 1971 ACI Code to incorporate the simpler of these two methods are suggested.

Keywords: building codes; columns (supports); concrete slabs; connections; flat concrete plates; lightweight aggregate concretes; moments; reinforced concrete; reinforcing steels; research; shear strength; shear tests; structural design; torsion.

ACI Member Neil M. Hawkins is associate professor of civil engineering, University of Washington, Seattle. He was formerly a Development Engineer with the Portland Cement Association. Dr. Hawkins is chairman of ACI Committee 355, Anchorage to Concrete, and a member of ACI Committees 215, Fatigue of Concrete; 426, Shear and Diagonal Tension; 443, Concrete Bridge Design; and 512, Precast Concrete. In 1970 he and Dr. Corley were corecipients of the ACI Wason Medal for research.

ACI Member W. Gene Corley is Manager, Structural Research Section, Portland Cement Association, Research and Development Division, Skokie, Illinois. In April 1970 he and Dr. Hawkins were corecipients of the ACI Wason Medal for Research. Currently, Dr. Corley is Chairman of ACI Committee 443, Concrete Bridge Design, and a member of ACI-ASCE Committee 428, Limit Design; and 545, Concrete Railroad Ties.

BACKGROUND

A series of investigations was initiated at the PCA Laboratories in 1965 to examine the strengthening of flat plate-column junctions by special shearhead reinforcement. In 1968 results were reported(1) of tests on 21 concentrically loaded slab-column specimens, 16 of which contained shearheads. Those results were used to develop the shearhead design criteria for interior column locations contained in Section 11.11 of ACI 318-71 (2).

The tests showed that once inclined cracking developed in the slab adjacent to the connection, all subsequently applied shears were carried by the shearhead. Failure was initiated either by punching along a surface following the perimeter of the shearhead or by exhaustion of the flexural capacity of the shearhead at the column face. To cover the first possibility, 11.11.2.3 specifies a critical design section that is dependent on the projection of the shearhead arms. The maximum shear stress is limited to $4\sqrt{f'_c}$ as for a concentrically loaded connection. To cover the second possibility, 11.11.2.2 specifies a minimum flexural capacity for the shearhead.

In many situations, a flat plate connection transfers moments as well as shears. Design criteria for connections without shearheads are specified in Section 11.13 of ACI 318-71. Those provisions presume that, for square columns, 60 percent of the moment is transferred across the critical section for shear by flexure and 40 percent

by eccentricity of the shear. Shear stresses are taken as varying linearly about the centroid of the critical section. The maximum shear stress is again limited to $4\sqrt{f'_c}$ Thus the shear which can be transferred to the column decreases linearly with increase in the moment transferred to the column. These criteria were based on the work of Hanson and Hanson, (3) who used all available test data to determine a reasonable value for the percentage of moment transferred by shear.

In 1971 the authors (4) proposed a refinement to the ACI Code procedure for the analysis of connections transferring moments. They suggested that the strength could be determined from the capacity in combined moment, shear, and torsion of the slab sections framing into each column face. This "beam analogy" gives good agreement with Hanson and Hanson's data and also predicts the strengths observed in tests on flat plate slabs supported on four corner columns (5). For that biaxial bending situation, the observed strengths were four times those predicted by the use of the ACI 318-71 provisions.

TEST PROGRAM

Test Specimens

Fourteen slab edge column specimens were made and tested. Details of a representative specimen are shown in Fig. 1. In the following discussions, the short dimensions of the slab are termed the "x" direction, and the long dimensions the "y" direction. The principal features of each test specimen are listed in Table 1.

The main variables were the proportions for the shearhead and the width of the column face in the x direction. The specimens were intended to represent the details of a flat plate structure in the vicinity of an exterior column. The dimensions and reinforcement were intended to represent those of a prototype design by the Empirical Method of Section 2104 of ACI-63 for columns at 20 ft. (6.1 m) centers and a live load of 100 lb/sq. ft. (490 kg/sq. meter).

Slab reinforcement consisted of No. 5 bars at 5-in. (12.7 cm) centers in both directions for the top mat and No. 4 bars at 6-in. (15.2 cm) centers in both directions for the bottom mat. Minor variations were made in these spacings in the vicinity of the column to avoid the column bars and to always provide two bars passing into the transverse column face, c_2. The effective depths for negative moments were 5-1/16 in. (12.7 cm) and 4-7/16 in. (11.3 cm) for bars in the y direction and x direction respectively.

All shearheads were T-shaped and made from combinations of American Standard I and Channel sections. A completed shearhead is shown in Fig. 2. When the shearhead arm consisted of two sections, its outside to outside width was 7 in. (17.8 cm), except for the arm in the x direction for specimens DC1 and DC2. For those arms, the structural shapes were positioned outside instead of inside the column bars, and the clear spacing between shapes was 5-1/4 in.

Materials

Properties of the concrete and reinforcement are listed in Table 1. Lightweight aggregate concrete with a 50 percent replacement of lightweight fines by normal weight sand was used for all specimens. This aggregate is designated as S14 in previous investigations (1) (6) (7). Concrete strengths were determined from tests on standard 6 x 12-in. cylinders.

Properties for the reinforcing bars were determined from tensile tests. All bars had yield stresses near those required for ASTM Designation A615, Grade 60, (8) and all had well defined yield plateaus. Properties for the shearhead were determined from tensile test coupons and from compressive tests of 5 in. (12.7 cm) long specimens. Yield strengths for webs and flanges were similar and results for compressive and coupon tests were in close agreement. The steel met the requirements of ASTM Designation A36 (9).

Test Procedure

The specimens were fabricated and tested employing procedures generally used in the PCA Structural Laboratory (10) (11). The test setup is shown in Fig. 3. To simulate the axial load in the prototype, the column was prestressed through a centrally located duct to the laboratory floor with a force of approximately 60 kips (132 kg).

Equal vertical downward loads were applied to the slab at five locations spaced at 3 ft. (91 cm) intervals around the perimeter of the slab. To maintain zero moment at the base of the column and to balance the moments transferred to the column, a horizontal restraining force equal to one of the vertical downward loads was applied at a point located 51 in. (129 cm) above the upper surface of the slab. Loads were applied by a hydraulic system and monitored by load cells mounted at one end of each loading rod. About ten increments of load were applied to each specimen to reach the ultimate load.

Electrical resistance gages were used to measure strains on the bottom surface of the slab adjacent to the column, on the reinforcing bars and on the shearhead arms. Deflections on the upper surface of the slab and horizontal displacement of the column were measured. In addition, rotations of the slab over a 10-in. (25 cm) gage length extending in the x direction from the center of the transverse column face were determined.

TEST RESULTS

Specimens exhibited four definable stages of behavior characterized with increasing load by: (1) flexural cracking at the column face parallel to the edge, (2) inclined cracking, (3) yielding of the top bars parallel to the direction of unbalanced moment, and (4) ultimate load. Yield strain was not observed for any of the top bars placed in the y direction.

Test results are summarized in Table 2. Inclined cracking loads were determined from strain measurements. This cracking occurred at about 60 percent of the ultimate load. Yielding of the top bars passing into the transverse column face occurred before or simultaneously with ultimate load. For specimens with heavy shearheads, crushing occurred at the junction of the bottom surface of the slab and the transverse face of the column well in advance of ultimate load. This crushing caused no marked change in the response of the specimens. Ultimate load was reached when a combination of a punching action at the transverse column face and a twisting fracture at the side faces occurred. This resulted in a sudden, rigid body rotation of the slab relative to the column.

Deflections

Load-deflection curves for all specimens are shown in Fig. 4. Deflections were measured at the center of the long side opposite the column. The curves in Fig. 4 were obtained using an x-y recorder. These results are not corrected for column rotations.

It is apparent that for specimens without a shearhead or with an inadequate shearhead, the punching failure occurred at the maximum load and the capacity dropped abruptly. As the adequacy of the shearhead increased, the loads for yield of reinforcement for ultimate load increased proportionately until, for a heavy shearhead, there was a pronounced plateau. This behavior is desirable where ductility of the slab-column junction is needed.

In the CH series, the main variable was the length of the

shearhead arm. The collapse loads increased with increasing lengths up to a maximum for CH3. Specimen CH4 contained a shearhead 20 percent longer. Although its collapse load was slightly less than for CH3, the specimen exhibited a marked yield plateau prior to collapse, and its overall behavior was more desirable.

Except for the width of the transverse column face, the specimens in the DC series were similar in most respects to specimens CN1, CC4, and CC5. Consequently, except for a reduction factor of about 10 percent on the loads, the load-deflection curves for the DC series are similar to those for the CC series.

The torsional characteristics of the shearhead had little effect on capacity. Specimens CC4 and CC5 had the torsion arms battened together, as shown in Fig. 2, to insure the development of a strong space truss. These specimens showed little improvement in characteristics relative to CC2 with non-battened arms.

The shearheads significantly increased the post-punching strengths. Those strengths were verified as repeatable by completely unloading and then reloading the specimen as indicated by broken lines in Fig. 4 for representative specimen CC4. For a slab without a shearhead the post-punching strength was about 55 percent of the punching strength. This percentage increased as the length and strength of the shearhead increased and reached about 80 percent for specimens CH4 and CC4.

Shearhead Forces

A measure of the magnitude and distribution of the bending moment, shear, and axial force in each shearhead arm was obtained from strain gages. Values for the arm in the x direction are listed in Table 2. Moments and axial forces were a maximum at the column face while shear reached maximum a short distance in front of this face. Provided the moment in the shearhead arm reached 95 percent of the plastic moment capacity, M_p, the ultimate loads increased with increasing M_p values. However, the change in capacity with M_p decreased as the M_p values increased. For those specimens in which the moment reached 95 percent of M_p, the axial force in the shearhead at ultimate load was generally less than the maximum observed at lower loads.

For the shearhead arms in the y direction, torsional effects

caused irregular variations in strains along the length and over the depth of each arm. Where the arms projected 15 in. (38 cm) or more, local yielding was recorded in the top flange of the arm closest to the transverse column face. However, the moments at collapse were always substantially less than M_p.

Crack Patterns

The crack patterns and failure surface for the representative specimen CC2 are shown in Fig. 5. Cracking showed four stages of development common to all specimens. The first load increment of about 6 kips caused flexural cracking at A shown in Fig. 5, across the width of the transverse column face. The second increment of about 3 kips initiated "flexure torsion" cracks, B, at the outer edge of the slab. The third increment, again of about 3 kips, resulted in crack C joining cracks A and B. Finally, when the applied load reached about 16 kips, crack D developed along almost the complete length of the reinforcing bar immediately in front of the column. This crack divided the slab into two zones in which clearly different crack patterns developed with further loading. In the torsion zone between this crack and the outer edge of the slab, additional torsional cracks developed outside of crack C. In the bending zone, cracks spread in a fan-like manner from the center of crack D.

For specimens without shearheads, the flexure-torsion cracks had spread over the full depth of the outer edge of the slab by the end of the third load increment. As the adequacy of the shearhead increased, the rate of development of these cracks decreased. Strain gages indicated inclined cracking was developed at about the load for full development of this crack.

Shortly before failure horizontal cracks, E, developed across the full width of the outer face of the column. For specimens without shearheads, the torsion crack, F, on the bottom surface of the slab extended toward the front corners of the column. As the adequacy of the shearhead increased, the development of this torsion crack was progressively retarded. For specimens with heavy shearheads, the front corners of the column spalled off simultaneously with the development of crack E. For specimens CC5 and DC2 with the heaviest shearheads, crushing developed over the full width of the column face prior to collapse.

Strains and Crack Widths

After flexural cracking and before the development of inclined cracking, the concrete and steel strains showed that the

behavior was essentially flexural. Strains and crack widths increased almost linearly with increasing load. Concrete strains were uniform across the width of each column face. Along the y axis, steel strains for bars in the x direction dropped off rapidly with increasing distance from the column. In contrast along the x axis, steel strains for bars in the y direction were practically constant from the center of the side face to the midpoint of the slab. Strains in the compression reinforcement were negligible.

An abrupt change in the relative rates at which concrete and steel strains developed occurred at about half the ultimate load. The load for that change is recorded as the inclined cracking load in column 2 of Table 2. The strain readings showed that inclined cracks formed initially in the plane of the slab adjacent to the transverse column face. For two specimens DN1 and CC5 the occurrence of cracking was substantiated by precise measurements of the changes in slab thickness adjacent to the transverse column face.

After inclined cracking, torsional effects became pronounced. The torsion crack at the outer edge opened rapidly with increasing load, and at the side face of the column, the concrete strains in the y direction increased at the outer edge and decreased at the inner face. Strains increased rapidly in the compression reinforcement adjacent to the column and in the tensile reinforcement close to the end of the shearhead arm extending in the x direction.

Failure Surfaces

Failure surfaces were revealed by breaking the slabs apart along their line of least resistance.

For specimens without shearheads, the surface at the transverse column face was similar to that for a shear failure under balanced loading (1). At the side faces, the surfaces were irregular and crossed by a series of torsion cracks.

For specimens with shearheads, the surfaces showed differing characteristics at the transverse and side faces of the column. At the transverse face, the shearhead was either "under-reinforcing" or "over-reinforcing" in the manner described previously for concentric loading (1). For an over-reinforcing shearhead, the failure surface followed the perimeter of the arm parallel to the direction of unbalanced bending. For an under-reinforcing shearhead, the surface fell well inside the end of the arm and did not differ materially from that for a specimen without a

shearhead. Specimen CC2 shown in Fig. 5 contained a shearhead that provided almost balanced reinforcement.

For the side faces, the effect of the shearhead depended primarily on its length. For all specimens, the critical torsion crack extended backwards from the transverse column face at an inclination of about 45^{o}. A long shearhead arm was crossed by this crack and twisting of the arm occurred unless the sections in it were battened together. For a long arm, the shearhead increased the ultimate torsional moment because it reduced the shear carried by the concrete. For the short shearhead arm, the torsion crack passed around its end and the effect of the arm was small.

ANALYSIS OF RESULTS

Three considerations are basic to interpretation of the implications of the test data. First, the contribution of the shearhead to the flexural strengths must be assessed. Second, a procedure is needed for predicting the observed shear strengths. Third, an evaluation must be made of the factors governing the strength of the shearhead.

Flexural Capacity

Previous work has shown that, for connections subject to balanced moment, the shear stress at failure decreases as the ratio of the measured strength V_{TEST} to the flexural capacity V_{FLEX} increases (12).

The yield line pattern for Specimen CN1 is shown in Fig. 6. The collapse load for this pattern is only slightly less than that for the slab failing as a wide beam about the x-x axis. Therefore, this wide beam concept was used to evaluate flexural strengths and an allowance made for the shearhead arm perpendicular to the edge by adding its plastic moment capacity to the moment capacity of the slab.

Ratios of V_{TEST} to V_{FLEX} are listed in Column (3) of Table 3. The measured strengths are all considerably less than the flexural strength. Ratios increase somewhat with increasing shearhead length from 0.37 for slabs without shearheads to 0.55 for slabs with long shearheads. These ratios are considerably less than those for the slab-column specimens tested by Hanson and Hanson (3).

Shear Capacity

Extrapolation of 1971 ACI Code procedure - Chapter 11 of the ACI Building Code (318-71) contains provisions for calculating shear strengths of slabs where moments are transferred to columns. Also, provisions for design of shearhead reinforcement are given. However, the Code specifically prohibits the combined use of these two provisions.

Where shearhead reinforcement is provided, the critical section for shear is taken through the shearhead arms at a location three-fourths of the distance from the face of the column to the end of the shearhead. The section is taken no closer than d/2 to the column perimeter. These sections for an edge column are shown in Fig. 7.

Where transfer of moment occurs, shear stresses are assumed to vary linearly about the critical section. The resultant distribution for an edge column with a long shearhead is shown in Fig. 8. The maximum shear stress occurs where the critical section crosses the shearhead arm. This stress is the sum of a uniform stress v_1 caused by the shear V, and a twisting stress v_2 caused by the transfer of the moment M. The width of the section under maximum stress can be relatively small. In contrast, for a specimen without a shearhead, this stress extends across the full width of the face BC.

For shears and moments transferred as indicated in Fig. 8 across the critical sections shown in Fig. 7, the ratios of measured shear strength to calculated shear strength, neglecting the limitation imposed by Section 13.2.4 of ACI 318-71 with respect to flexural stresses, are as listed in column (4) of Table 3. A maximum shear stress of $0.6f_{ct}$, the Code value for lightweight aggregate concrete, was used to calculate strengths. The values f_{ct} were taken as $A\sqrt{f'_c}$ where A was the average value for the coefficient of proportionality between the measured splitting strength f_{sp} and $\sqrt{f'_c}$. In all cases, calculations were based on measured material properties.

While the Code procedures result in reasonable predictions of the strengths for specimens with short shearheads, they overestimate strengths for specimens with long shearheads as shown in Fig. 9. Consequently, a modification of this extrapolation of the 1971 ACI Code is needed.

Modification of 1971 ACI Code (ACI 318-71) -- For a specimen with a short shearhead, the critical torsion crack passed outside the end of the arm in the y-direction. This observed behavior suggests that the critical section can be idealized as shown in Fig. 7 (2). However, for a long arm, the critical torsion crack stayed close to the column. In that case, it was observed that, although the torsion arm was effective for transferring shear, it was not effective for torsion. Therefore, the critical section shown in Fig. 7 (1) is more appropriate for calculations of the shear stresses caused by the transfer of moments. Then even though the critical sections for v_1 and v_2 differ, they coincide or are in close proximity at the column corners where the failures initiated. Therefore, since a long shearhead attracts most of the shear as it funnels toward the column, it is reasonable to take the maximum shear stress as the sum of the two components v_1 and v_2.

Ratios of measured shear force to calculated shear force based on a maximum shear stress to $0.6f_{ct}$ are as listed in column (5) of Table 3. The sections shown in Fig. 7 were used, as appropriate, to determine the shear stress caused by the shearing forces, but, the section shown in Fig. 7 (1) was always used to determine the shear caused by the transfer of moments. That moment was taken as the moment on the column less the moment transferred by eccentricity of the shearing force. With this modification to the Code provisions, ratios of calculated to measured strengths are as shown in Fig. 9. The procedure results in the same conservatism for all shearhead lengths. Considering the limited test data available, the useful length of $(\ell_v - c_1/2)$ should be limited to 4.0d.

Beam analogy -- In a previous paper, the authors proposed a "beam analogy" for calculating the strength of connections transferring unbalanced moments (4). These test results provide additional evidence that this approach to design is applicable.

Use of the "beam analogy" requires knowledge of the shear and moment distributions around the column. The shear distribution at ultimate load can be established from the potential yield line pattern and the assumption that the applied loads will be transmitted to the column by the stiffest available path. For the yield line pattern shown in Fig. 6, the loads at points 1 and 3 flow directly to the column via the elements on which they act. Further, since a slab is stiffer in bending than in torsion, the load at point 2 will be transmitted across the yield line BH to the face BC rather than across line BF to the face AB.

Experimental evidence that this assumption is reasonable is given in Appendix II.

For a specimen without a shearhead, the beam analogy (4) predicts two possible strength limits for a connection at an edge column. For moment-torsion interaction, the capacity is dictated by the sum of the torsional strengths of the beam sections of width $(c_1 + d_2/2)$ at the side faces and the flexural strength of the section of width (c_2+d_1) at the transverse face. For shear-torsion interaction, the capacity is dictated by the shear strength of the section at the transverse face and the torsional strengths of the sections at the side faces. Calculations of these strengths for specimen DN1 are given in Reference 4.*

For a specimen with a shearhead, strength may still be governed by either of these modes. In addition, failure can occur either in shear or bending on a section passing outside the shearhead arm extending in the x-direction. Therefore, four separate strength calculations are necessary for each specimen.

Ratios of measured to computed strengths for moment-torsion interaction, V_{MT} and V_{MTS}, are listed in columns (6) and (7) of Table 3 and strengths for shear-torsion, V_{ST} and V_{STS}, in columns (8) and (9). For the strengths V_{MT} and V_{ST} the critical sections are essentially the same as those shown in Fig. 7 (1) for specimens without shearheads. For V_{MTS} and V_{STS} the critical sections are those shown in Fig. 7(2) and 7(3) except that for V_{MTS} the section is taken as extending to the end of the arm in the x direction.

For the reasons discussed in Ref. 4, the torsional strengths of the side faces were based on the capacity T_o of a plain concrete section of width $(c_1 + c_2/2)$ failing about the smaller cross-sectional dimension. To account for shear this capacity was reduced to T in accordance with the expression:

$$T = T_o \sqrt{1 - \left(\frac{V}{V_o}\right)^2} \quad \ldots\ldots\ldots\ldots\ldots\ldots (1)$$

where

V = shear carried by the concrete at the face AB

V_o = shear strength of the face AB, excluding shearhead

---

*Slabs numbered CN1S14 and DN1S14 in Reference 4 correspond to CN1 and DN1, respectively, in this paper.

Where the shearhead did not extend a distance 1.5d beyond the critical section, the shear V was taken as $(1-\alpha_v)$ times the ultimate shear at face AB. The relative stiffness, α_v, is the ratio of shearhead stiffness to that of a cracked concrete section as described in Appendix I. Where the shearhead extended further than 1.5d, V was taken as $(1-\alpha_v)$ times the shear at face AB at inclined cracking. The measured torques, determined as indicated in Appendix II, averaged 9 percent higher than the torques predicted by Eq. (1).

Flexural capacities of the sections at the transverse face were calculated assuming complete yielding of the tension, compression, and shearhead reinforcement and an ultimate stress of $0.85f'_c$ over the depth of the compressed concrete.

If the strength V_{MT} governs, then the moment on the critical section is less than the static moment on the line x-x in Fig. 6 by an amount equal to the moment transferred by the eccentricity of the shear on the critical section. The moments transferred by shear were computed assuming that the loads on element FGKL in Fig. 6 caused shear stresses uniformly distributed over the length of the critical section between points B' and C' in Fig. 7(2).

The strength V_{ST} governs if the shear stress on the concrete for the width $(c_1 + d_1)$ exceeds $0.6f_{ct}$. The shear on the concrete was computed assuming the capacity of the shearhead was limited to M_P. The strength V_{STS} governs if the shear stress on the critical section between points B' and C' in Fig. 7(2) exceeds $0.6f_{ct}$. Shear stresses were assumed to be uniform along the length B'C'.

For each specimen listed in Table 3, the ratio for the lowest strength predicted by the beam analogy is enclosed in parentheses. For all specimens except DN1 without a shearhead, moment-torsion interaction dictated the strength. The capacity is governed by conditions at the column face for long shearheads and by conditions on the critical section extending to the end of the shearhead arm for short shearheads. These patterns imply increasing ductilities for increasing shearhead lengths.

Ratios of measured to calculated strengths average 1.26 for the modified code procedure and 1.04 for the beam analogy. Appendix III contains shear strength calculations for representative Specimen CC2.

Shearhead Moment Capacity

The load-shear relationships described in Appendix II indicate that the distribution of shear in the shearhead at collapse can be idealized as shown in Fig. 10. Shear at ultimate on one column face is V_{u1}, the total shear minus the shear on faces other than the one considered. The inclined cracking shear for the area tributary to a given column is V'_c. Based on the assumption that V'_c is half V_{u1}, the following equation is obtained for the moment at the face of the column at ultimate load:

$$M_s = \frac{V_{u1}}{2}\left[h_v + \alpha_v\left(\ell_v - \frac{c_1}{2}\right)\right] \quad \ldots\ldots\ldots (2)$$

The shearhead will have an adequate capacity if its plastic moment M_p exceeds M_s. Otherwise, the ultimate shear, V_{u1}, must be limited to the value for M_p less than M_s.

Values of the moment at collapse calculated from Eq. (2) for the arm in the x direction are compared in Table 3 with the measured moment determined from the strain gages on that shearhead arm. For Specimen CT1, the moment M_s calculated from Eq. (2) exceeded M_p, therefore M_s was limited to M_p. The shear values used in Eq. (2) were determined from the shear distributions obtained using the modified code procedure since the tributary shears for this distribution were slightly higher than the shears for the beam analogy. It is apparent that for either method of analysis Eq. (2) can be used to predict values of the moment in the shearhead or the capacity required for this shearhead.

RECOMMENDATIONS

These test results show that shearhead reinforcement is effective in increasing the ultimate shear capacity and ductility of connections between thin slabs and edge columns. Based on the results of the 14 tests reported here, the design procedure for shearhead reinforcement consisting of structural shapes, Section 11.11 of the 1971 ACI Building Code, should be modified to make it applicable when unbalanced moment must be transferred from slab to column. The following modifications of the 1971 ACI Code are suggested:

1. In Section 11.11.2, the prohibition against use of shearheads at edge or corner columns should be removed.

2. The required moment capacity, M_p, of each arm of the shearhead is given by Eq. (2) where M_s is taken equal to M_p. In Section 11.11.2.2, the term $V_u/8$ in Eq. (11-26) should be replaced by $V_{u1}/2$. In view of the limited available test data, the maximum length of shearhead arm considered effective should be $(\ell_v - \frac{c_1}{2}) = 4d$.

3. A requirement should be added that, when unbalanced moments are considered, the shearhead must have adequate anchorage to transmit to the column the moment M_p.

4. In Section 11.11.2.3, the critical design section to be considered effective for moment transfer should be the same as that at a column without a shearhead. Section 11.13 should be used to calculate the shear stresses caused by unbalanced moment.

5. For nominal weight concrete, the sum of the maximum shear stresses calculated for vertical shear and for unbalanced bending should be limited to $4\sqrt{f'_c}$ the value in 11.11.2.4 and 11.13.2.

6. In Section 11.11.2.5, the term $V_u/8$ in Eq. (11-27) should be replaced by the term $\frac{V_{u1}}{2}$.

Strong evidence is presented showing the desirability of a future modification of the Building Code to permit the use of a "beam analogy" for calculating the strength of connections at edge columns.

ACKNOWLEDGMENTS

This investigation was conducted in the Structural Laboratory of the Portland Cement Association. Dr. E. Hognestad, Director, Engineering Development Department, provided valuable guidance in arriving at the final design recommendations. Credit is due to B. J. Doepp, B. W. Fullhart, O. A. Kurvits, W. W. Maneck, and W. Hummerich, Jr. for their assistance in the fabrication and testing of the specimens.

REFERENCES

1. Corley, W. G. and Hawkins, N. M., "Shearhead Reinforcement for Slabs," ACI Journal, Proceedings V. 65, No. 10, October 1968, pp. 811-824. Also PCA Development Bulletin D144.

2. ACI Committee 318, "Building Code Requirements for Reinforced Concrete (ACI 318-71)", American Concrete Institute, Detroit, 1971, 78 pp.

3. Hanson, N. W. and Hanson, J. M., "Shear and Moment Transfer Between Concrete Slabs and Columns," Journal, PCA Research and Development Laboratories, Vol. 10, No. 1, January 1968, pp. 2-16. Also PCA Development Bulletin D129.

4. Hawkins, N. M. and Corley, W. G., "Transfer of Unbalanced Moment and Shear from Flat Plates to Columns," Paper SP30-7, Cracking, Deflection, and Ultimate Load of Concrete Slabs Systems, American Concrete Institute, Detroit, 1971, pp. 147-176.

5. Zaghool, E.M.F., de Paiva, H.A.R., and Glockner, P. G., "Tests of Reinforced Concrete Flat Plate Floors," Structural Division Journal, ASCE, Vol. 96, No. ST3, March 1970, pp. 487-507.

6. Hanson, J. A., "Replacement of Lightweight Aggregate Fines with Natural Sand in Structural Concrete," ACI Journal, Proceedings, V. 61, No. 7, July 1964, pp. 779-794. Also, PCA Development Bulletin D80.

7. Pfeifer, D. W., "Sand Replacement in Structural Lightweight Concrete - Splitting Tensile Strength," ACI Journal, Proceedings, V. 64, No. 7, July 1967, pp. 384-392. Also PCA Development Bulletin D120.

8. ASTM Designation: A615-68, "Standard Specification for Deformed Billet-Steel Bars for Concrete Reinforcement," ASTM Standards, Part 4, American Society for Testing and Materials, Philadelphia.

9. ASTM Designation: A36-67, "Standard Specification for Structural Steel," ASTM Standards, Part 4, American Society for Testing and Materials, Philadelphia.

10. Hognestad, E., Hanson, N. W. Kriz, L. B. and Kurvits, O. A., "Facilities and Test Methods of the PCA Structural Laboratory,"

Journal of the Portland Cement Association Vol. 1, No. 1, January 1959, pp. 12-20 and 40-44, Vol. 1, No. 2, May 1959, pp. 30-37; Vol. 1, No. 3, September 1959, pp. 35-41; PCA Development Bulletin D33.

11. Hanson, N. W., Hsu, T.T.C., Kurvits, O. A. and Mattock, A. H., "Facilities and Test Methods of PCA Structural Laboratory - Improvements 1960-65," Journal of the Portland Cement Association, Vol. 3, No. 2, May 1961, pp. 27-31, Vol. 7, No. 1, January 1965, pp. 2-9 and Vol. 7, No. 2, May 1965, pp. 24-38; PCA Development Bulletin D91.

12. Moe, J., "Shearing Strength of Reinforced Concrete Slabs and Footings Under Concentrated Loads," Development Bulletin D47, Portland Cement Association, April 1961, 130 pp.

APPENDIX I

NOTATION

a = depth of equivalent rectangular stress block

α_v = relative stiffness of shearhead to that of a composite section made up of a cracked section of the slab with a width equal to that of the column plus the slab effective depth and including the shearhead.

A = average value of coefficient of proportionality between measured splitting strength f_{sp} and $\sqrt{f'_c}$.

c_1 = width of column parallel to direction of applied moment, in.

c_2 = width of column perpendicular to direction of applied moment, in.

c_o = distance from edge of slab to center of shearhead, in.

d, d_1, d_2 = effective depths of tension steel, average, face c_1, face c_2 in.

e = eccentricity from column center of shear on critical section tributary to face BC, in.

f'_c = cylinder compressive strength of concrete, psi.

f_{ct} = average splitting tensile strength of lightweight aggregate concrete, psi.

f_{sp} = measured splitting tensile strength of lightweight aggregate concrete, psi.

h_v = depth of steel shape in shearhead, in.

ℓ_v = length of shearhead arm from center of column, in.

M_p = plastic moment capacity of shearhead, lb-in.

M_s = calculated maximum moment in shearhead, lb-in.

M_{TEST} = measured maximum moment in shearhead, lb-in.

T = torsional strength for face AB in combined bending, torsion, and shear, lb-in.

T_o = torsional strength for face AB in pure torsion, lb-in.

V = shear carried by concrete at face AB, lb.

V_{BEAM} = calculated load for governing condition by beam analogy, lb-in.

V'_c = shear at inclined cracking, lb.

V_{FLEX} = calculated ultimate load for flexural failure, lb.

V_{MT}, V_{MTS} = shear capacity for moment-torsion interaction at column face, around end of shearhead, lb.

V_o = shear capacity for face AB, excluding shearhead, lb.

V_{ST}, V_{STS} = shear capacity for shear-torsion interaction at column face, around end of shearhead, lb.

V_{TEST} = measured ultimate shear, lb.

V_u = ultimate shear, lb.

V_{u1} = ultimate shear on face considered, lb.

APPENDIX II

Load-shear relationships for the shearhead arms of Specimen CH4 are shown in Fig. A1. To obtain these relationships from measured strains, the shears were assumed constant over the intervals between gage lines. At loads less than the inclined cracking load, the broken line indicates the calculated relationship for full composite action. The calculated shear was taken as $\alpha_v V$ where V is the load on region FGKL in Fig. 6, and α_v is the relative stiffness of the shearhead to that of a cracked composite section of width $(c_2 + d_1)$ at the column face BC. For a load of 18 kips, $\alpha_v V$ equals 2.1 kips for the arm in the x direction. This value is in better agreement with the measured shears than is the value of 1.3 kips for shears uniformly distributed around the column.

For loads greater than the inclined cracking load, the broken line indicates the relationship if all the shears applied to region FGKL after inclined cracking are concentrated close to the column face BC. The test results are in close agreement with this relationship. Consequently, it appears that the action by which the shearhead carries shear is the same as that observed previously for balanced loading (1).

The distribution of moments also agreed with the concept that forces were transmitted to the column via the stiffest available load path. Shown in Fig. A2 are several examples of relationships between the total torsional moment on the side faces AB and CD in Fig. 6 and the static moment about the line x-x. The torsional moments were obtained by subtracting from the static moment the resisting moment for the width $(c_2 + d_1)$, including the shearhead. The resisting moment was calculated from the measured strains.

Figure A2 indicates that, except at loads near ultimate, the torque increased along with the static moment. However, the rate of increase was only half that for the static moment even though the resisting area in torsion was about 100 percent greater than the resisting area in flexure.

Except for specimens without shearheads or with short shearheads, the ultimate torsional moments were approximately the same for all specimens. The relationships in Fig. A2 are approximately those predicted if the twist per unit length, adjacent to the column of the element AEFB in Fig. 6 equals the curvature in pure bending for a section of width (c + d) at the transverse face BC. Further, it appears from Fig. A2 that when the maximum torsional moment is reached on the side faces, this resistance can be maintained for increasing static moments until the flexural capacity or shear capacity is reached.

APPENDIX III

Specimen CC2

Data: V_{TEST} = 37.4 kips; h = 3.0 in.; $0.6f_{ct}$ = 210 psi; M_p = 132 kip-in.;

α_v = 0.27

Maximum static moment transferred to column, M_t = 801 kip-in.

Load on element FGKL (Fig. 6) at failure, V_{BC} = 22.8 kips

Ultimate resisting moment for width ($c_2 + d_1$) of face BC; excluding shearhead, M_r = 230 kip-in., including shearhead, M_f = 420 kip-in.

(a) Shear Capacity by Code Provisions

In Fig. 8:

a = 9.38 in.; x = 18.28 in.; y = 13.75 in.; b = 7.0 in.

A = 339 in.^{2}; c_b = 11.87 in.; J = 25,900 in.^{4}

e = 9.75 in.; k = 0.35

$$v_1 = \frac{37.4 \times 1000}{339} = 110 \text{ psi}$$

$$v_2 = \frac{0.35 \times (801 - 37.4 \times 9.75) \times 1000 \times 11.87}{25,900} = 71 \text{ psi}$$

$$\frac{v_{max}}{0.6f_{ct}} = \frac{110 + 71}{210} = 0.86$$

(b) Shear Capacity by Modified Code Provisions

In Fig. 8:

v_1 = 110 psi as in (a)

For section 7(1) A = 216 in.^{2} c_{AB} = 4.53 in.; J = 5,196 in.^{4};
c_{CD} = 3.84 in.; k = 0.38

$$v_2 = \frac{0.38 \times (801 - 37.4 \times 9.75) \times 1000 \times 4.53}{5,196} = 146 \text{ psi}$$

$$\frac{v_{max}}{0.6f_{ct}} = \frac{110 + 146}{210} = 1.22$$

(c) Shear Capacity by Beam Analogy

Moment-Torsion, V_{MT} : T_o = 107.8 kip-in.; T = 97 kip-in.

Therefore $M_{CALC} = 2T + M_f + V_{BC} \times \frac{c_1}{2}$

$= 194 + 420 + 22.8 \times 6 = 751$ kip-in.

$$\frac{M_t}{M_{CALC}} = \frac{801}{751} = \frac{V_{TEST}}{V_{MT}} = 1.07$$

Moment-Torsion, V_{MTS}: Critical section tributary to face BC extends to L_{sx}

increase in eccentricity of V_{BC}, e', = 10.76 in.

$$M_{CALC} = 2T + M_r + V_{BC}\left(\frac{c_1}{2} + e'\right)$$

$= 194 + 230 + 22.8 \times 16.76 = 805$ kip-in.

$$\frac{M_t}{M_{CALC}} = \frac{801}{805} = \frac{V_{TEST}}{V_{MT}} = 1.00$$

Shear-torsion, V_{ST} Shear on concrete, $V_{co} = \frac{V_{BC}}{2}(1 - K)$

$$= \frac{22.8}{2} \times 0.73 = 8.33 \text{ kips}$$

Shear stress on BC, $= \frac{V_{co}}{(c_2 + d_1)d_2} = \frac{8.33 \times 1000}{(17.03)(4.44)} = 110$ psi

$$\frac{V_{TEST}}{V_{STF}} = \frac{\text{shear stress on BC}}{0.6f_{ct}} = \frac{110}{210} = 0.52$$

Shear-torsion, V_{STS}: Critical section tributary to face BC, extends to 3/4 L_{sx}

$$\text{Shear stress on B'C'} = \frac{V_{BC}}{\text{length B'C' x } d_2} = \frac{22.8 \times 1000}{35.2 \times 4.44} = 146 \text{ psi}$$

$$\frac{V_{TEST}}{V_{STS}} = \frac{\text{Shear stress on B'C'}}{0.6 f_{ct}} = \frac{146}{210} = 0.70$$

Conclude: Moment-Torsion governs

(d) Moment in Shearhead

By modified code provisions: Length of critical section for direct shear tributary, to BC = 32.8 in. ($b + 2\sqrt{x^2 + y^2}$ - Fig. 8)
From (b) $v_1 = 110$ psi; $v_2 = 146$ psi

Shear force due to direct shear - $v_1 \times 32.8 \times d$

$$= \frac{110 \times 32.8 \times 4.75}{1000} = 17.1 \text{ kips}$$

Length of critical section for moment transfer tributary to BC = 16.75 in ($c_2 + d$)

Shear force due to moment transfer $= \frac{146 \times 4.44 \times 16.75}{1000} = 10.9$ kips

in Eq. (2):

$$V_u = 17.1 + 10.8 = 27.9 \text{ kips}$$

$$M_s = \frac{27.9}{2} \times (3.0 + 0.27 \times 20.88)$$

$$= 121 \text{ kip-in.} < M_p = 132 \text{ kip-in.}$$

$$\frac{M_{TEST}}{M_s} = \frac{132}{121} = 1.09$$

By beam analogy

$$V_u = V_{BC} = 22.8 \text{ kips}$$

$$M_s = \frac{22.8}{2} \times (3.0 + 0.27 \times 20.88)$$

$$= 99 \text{ kip-in.} < M_p = 132 \text{ kip-in.}$$

$$\frac{M_{TEST}}{M_s} = \frac{132}{99} = 1.33$$

TABLE 1 - PROPERTIES OF TEST SPECIMENS

Mark	Cylinder Strength		Slab Reinf. Yield Stress		Shearhead					
	Compress.	Splitting Tension	Negative	Positive	Position	Perpendicular to Edge			Parallel to Edge	
						Type	Proj. $\ell_v - \frac{c_1}{2}$	Yield Stress	Type	Proj. $\ell_v - \frac{c_2}{2}$
	f'_c psi	f_{sp} psi	ksi	ksi	c_o in.		in.	ksi		in.
CN1	3290	344	64.5	66.6	-	None	-	-	None	-
CH1	3370	325	64.2	67.2	8.44	3I5.7	8.44	47.8	3I5.7	6.0
CH2	3350	332	64.7	67.7	8.44	3I5.7	11.44	47.8	3I5.7	9.0
CH3	3120	343	64.6	67.5	8.44	3I5.7	14.44	47.8	3I5.7	12.0
CH4	3640	326	64.2	66.8	8.44	3I5.7	17.44	47.8	3I5.7	15.0
CT1	3600	326	64.9	66.8	8.50	3T2.4*	14.50	43.0	3T2.4*	15.0
CC1	3350	370	57.6	61.3	3.56	2 3[5.0	21.06	44.0	3I5.7	15.0
CC2	3300	385	57.6	62.0	5.88	2 3[5.0	20.88	44.0	2 3[5.0	15.0
CC3	3230	375	57.3	61.7	5.88	2 3[4.1	14.88	43.0	2 3[4.1B**	9.0
CC4	3390	377	57.6	62.7	5.88	2 3[4.1	17.88	39.0	2 3[4.1B**	12.0
CC5	3700	364	57.1	61.3	5.88	2 3I5.7	20.88	46.0	2 3[4.1B**	15.0
DN1	3280	358	57.0	61.6	-	None	-	-	None	-
DC1	3130	384	57.1	61.9	5.88	2 3[4.1	14.88	43.0	2 3[4.1B**	11.0
DC2	3480	351	57.6	61.7	5.88	2 3I5.7	20.88	46.0	2 3[4.1B**	17.0

* Fabricated by splitting 8 Jr. 5.5 beam

** B Channels battened together

TABLE 2 - TEST RESULTS

Mark	Inclined Cracking	Load				Shearhead Perpendicular to Edge				
		Yielding		Crushing	Ultimate V_{TEST}	Full Plastic Moment	Max. Moment M_{TEST}	Max. Shear	Max. Axial Force	Axial Force at Ultimate Load
		Reinf.	Shear-head							
	kips	kips	kips	kips	kips	kip-in.	kip-in.	kips**	kips	kips
CN1	14.5	25.0	-	-	25.0	No shearhead				
CH1	16.8	28.6	-	-	28.6	91.8	50.5	-	4.6	3.7
CH2	17.6	30.4	-	-	30.4	91.8	62.4	8.9b	22.8	22.8
CH3*	-	-	-	-	33.5	91.8	-	-	-	-
CH4	20.7	31.6	28.5	25.8	32.5	91.8	91.0	9.2b	19.8	18.6
CT1	15.4	28.4	15.4	24.1	28.6	24.6	24.6	5.0a	6.5	0.0
CC1	21.0	31.7	25.9	31.3	35.4	132.0	126.0	9.6a,b	39.6	21.0
CC2	20.6	33.4	25.6	33.2	37.4	132.0	132.0	12.1a	24.4	2.0
CC3	18.0	32.7	30.7	28.0	33.2	112.0	102.0	18.6b	20.0	20.0
CC4	20.7	33.6	25.8	31.0	35.0	103.0	103.0	8.9a	20.0	17.1
CC5	20.6	38.1	38.1	30.4	39.1	176.6	173.0	14.3b	34.2	34.2
DN1	12.9	22.2	-	-	22.7	No shearhead				
DC1	18.4	30.1	-	28.5	30.7	112.0	85.0	6.8b	14.3	14.3
DC2	20.7	31.5	33.3	28.0	37.1	176.6	151.0	11.8b	8.0	58.0

* Insufficient loading increments for determination of additional information.

** a: maximum shear 3-4 in. from column face; b: maximum shear 6-8 in. from column face.

TABLE 3 - COMPARISON OF MEASURED AND COMPUTED STRENGTHS

Mark	Ultimate Shear V_{TEST} kips	$\frac{V_{TEST}}{V_{FLEX}}$	SHEAR CAPACITY						$\frac{M_{TEST}}{M_s}$
			Code Procedures		Beam Analogy				
			$\frac{V_{TEST}}{V_{CO}}$	$\frac{V_{TEST}}{V_{COM}}$	$\frac{V_{TEST}}{V_{MT}}$	$\frac{V_{TEST}}{V_{MTS}}$	$\frac{V_{TEST}}{V_{ST}}$	$\frac{V_{TEST}}{V_{STS}}$	
(1)	(2)	(3)	(4)	(5)	(6)	(7)	(8)	(9)	(10)
CN1	25.0	0.37	1.22	1.22	(1.04)**	-	0.94	-	-
CH1	28.6	0.40	1.34	1.32	0.92	(1.06)	0.43	0.98	0.97
CH2	30.4	0.43	1.30	1.31	0.97	(1.04)	0.46	0.91	1.00
CH3	33.5	0.48	1.20	1.37	1.06	(1.07)	0.52	0.90	-
CH4	32.5	0.44	0.87	1.12	(1.02)	0.96	0.47	0.72	1.17
CT1	28.6	0.41	0.83	1.05	(1.04)	0.87	0.63	0.72	1.00*
CC1	35.4	0.52	0.82	1.16	(1.01)	0.98	0.48	0.63	1.06
CC2	37.4	0.55	0.86	1.22	(1.07)	1.00	0.52	0.70	1.09
CC3	33.2	0.50	1.00	1.26	1.04	(1.06)	0.49	0.78	1.21
CC4	35.0	0.53	0.96	1.23	(1.06)	1.01	0.50	0.72	1.07
CC5	39.1	0.55	0.82	1.19	(1.04)	1.01	0.48	0.67	1.23
DN1	22.7	0.37	1.37	1.37	0.98	-	(1.00)	-	-
DC1	30.7	0.46	1.09	1.43	0.99	(1.03)	0.51	0.77	1.04
DC2	37.1	0.51	0.81	1.33	(1.06)	1.02	0.61	0.63	1.20

* M_s limited to M_p

** Parenthesis indicates lowest strength predicted by Beam Analogy

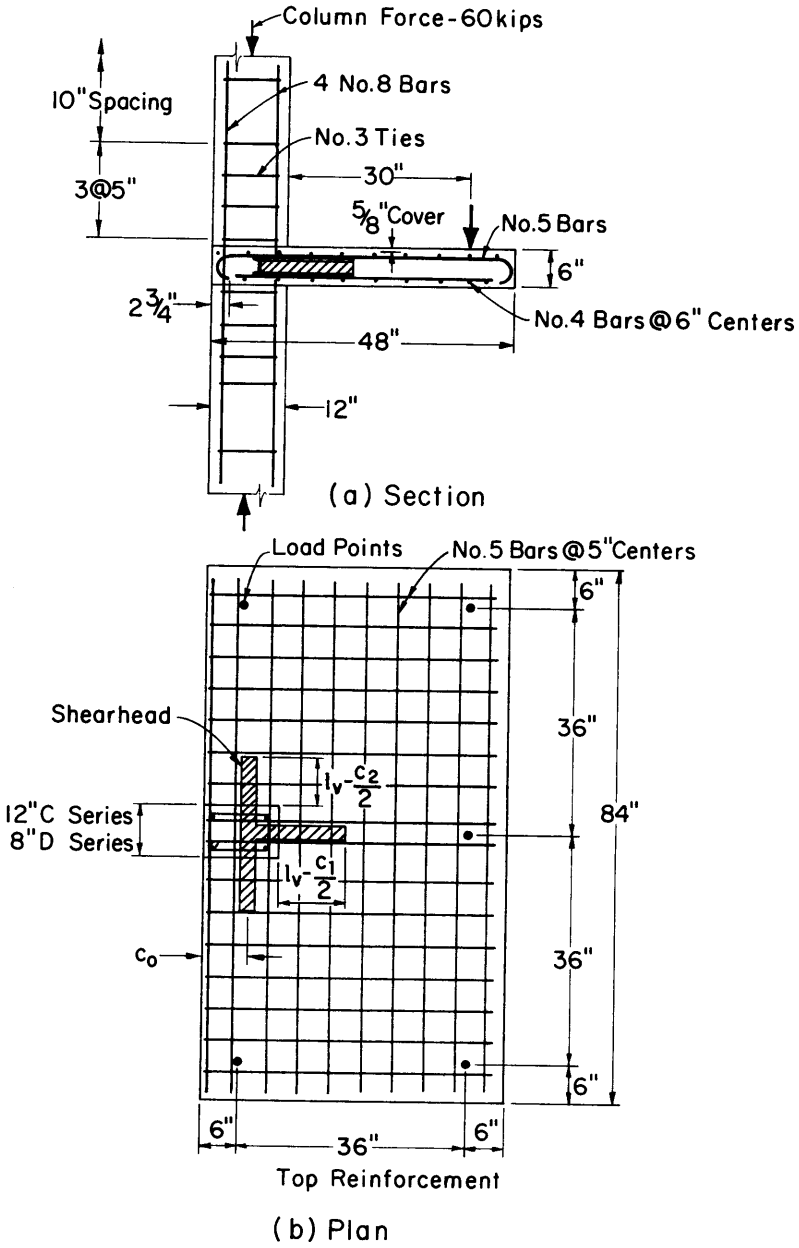

Fig. 1—Dimensions for Test Specimens

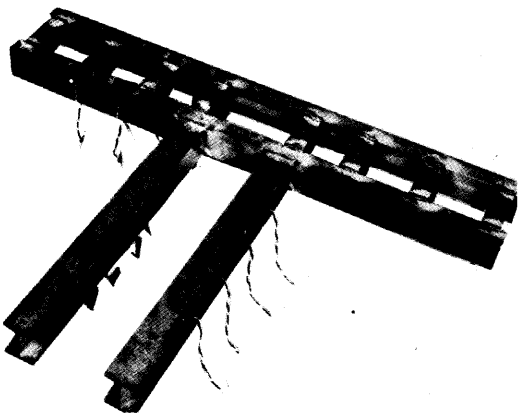

Fig. 2–Shearhead for Specimen CC5

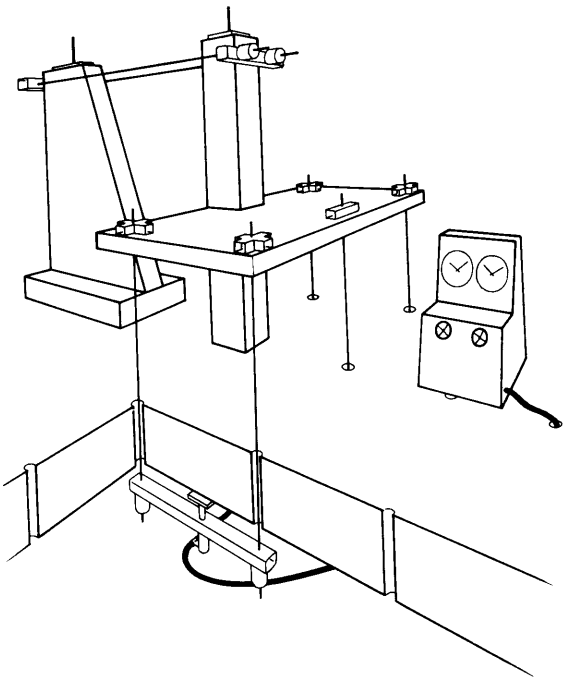

Fig. 3–Test Arrangement

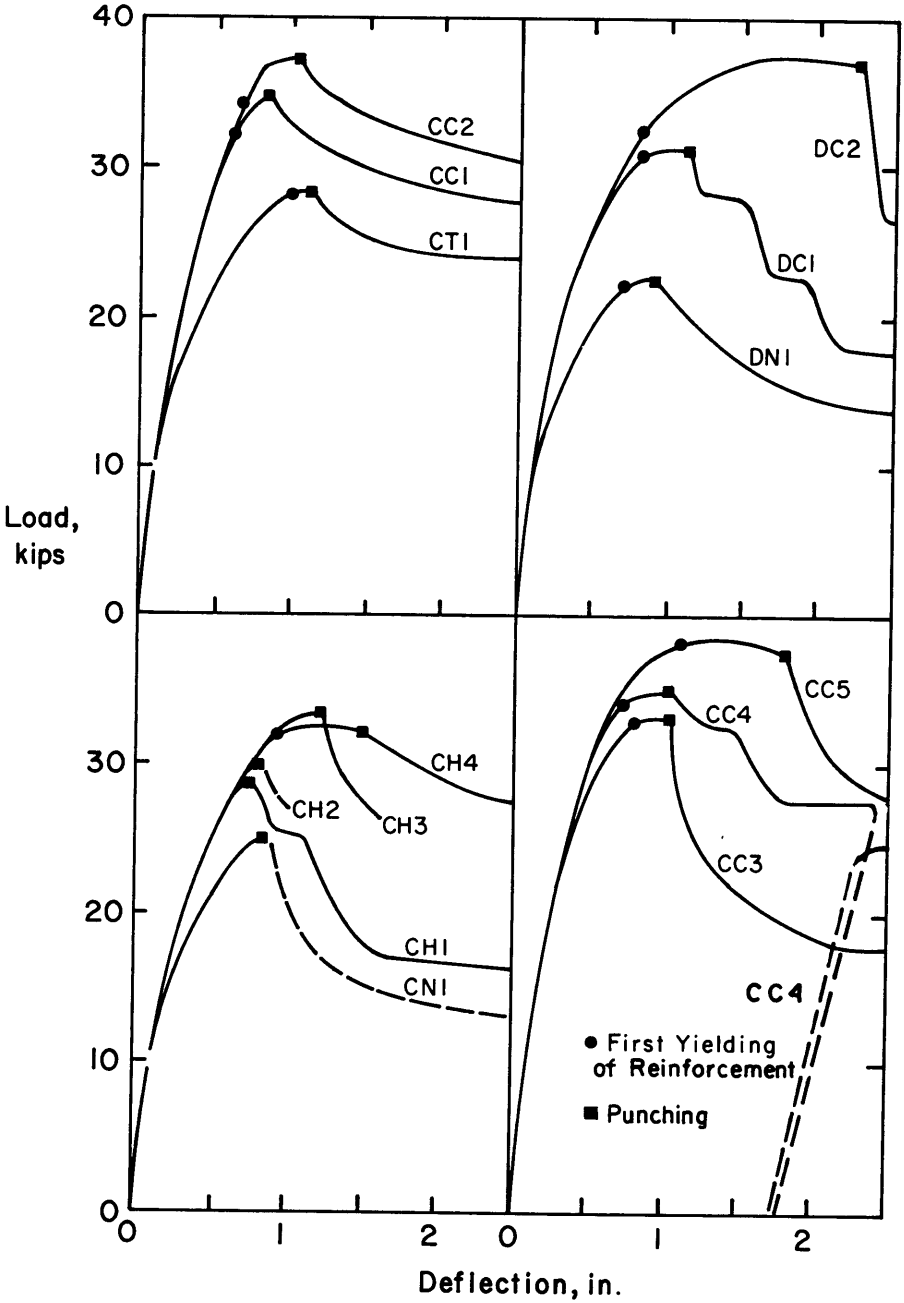

Fig. 4–Load-Deflection Curves

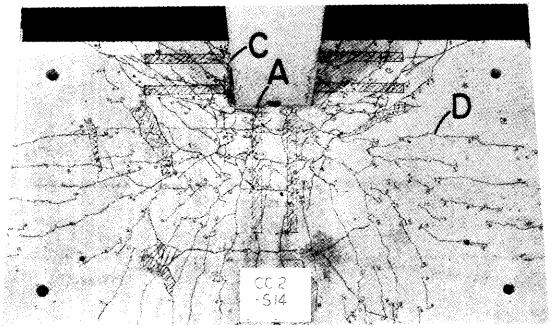

(a) Top of Slab

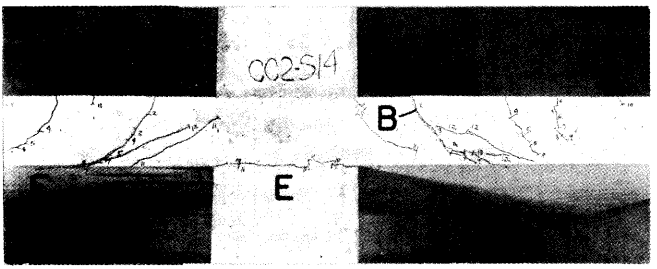

(b) Outer Edge of Slab

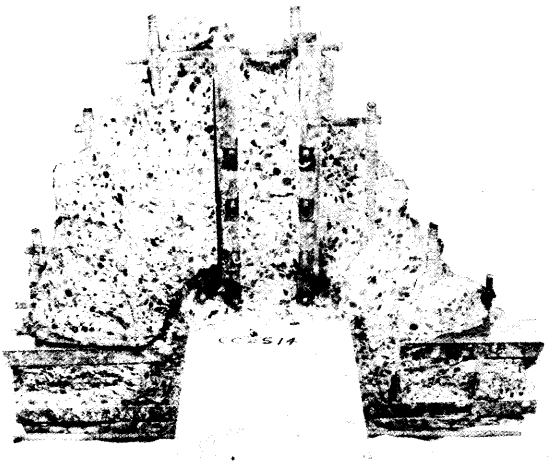

(c) Failure Surface

Fig. 5-Crack Pattern and Failure Surface for Specimen CC2

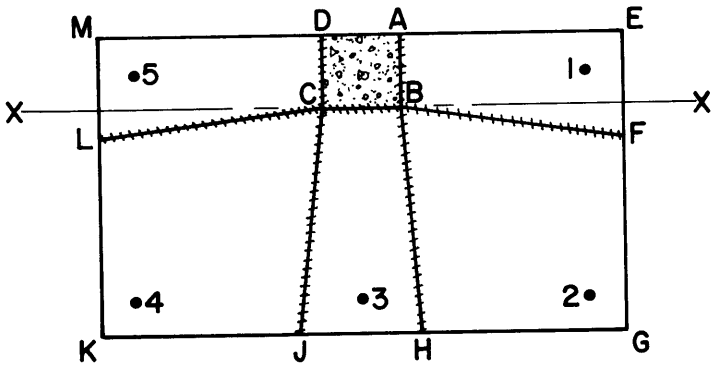

Fig. 6–Yield Line Pattern

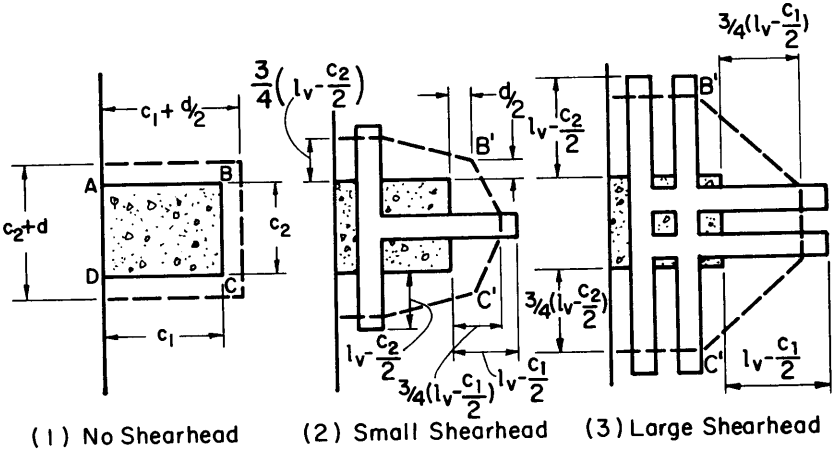

Fig. 7–Location of Critical Section

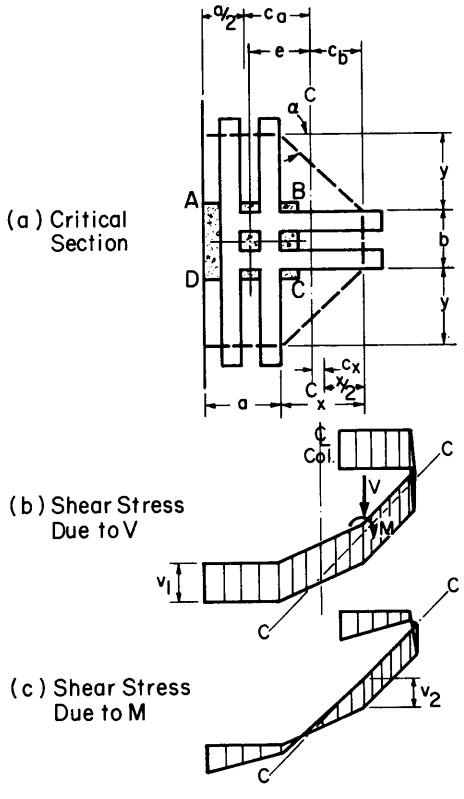

$$a+x-c_b = \frac{a^2+2\sqrt{x^2+y^2}(a+\frac{x}{2})+b(x+a)}{A_c}$$

$$v_1 = \frac{V}{A_c} = \frac{V}{(2a+b+2\sqrt{x^2+y^2})d}$$

where $k = 1-\frac{1}{1+\frac{2}{3}\sqrt{\frac{a+x}{b+2y}}}$

$$v_2 = \frac{kMc_b}{J}$$

$$J = \frac{a^3d}{6} + \frac{d^3a}{6} + \left[\frac{(x^2+y^2)^{\frac{3}{2}}d}{6} + d^3(x^2+y^2)^{\frac{1}{2}}\right]\cos\alpha + bdc_b^2 + 2(x^2+y^2)dc_x^2 + adc_a^2$$

Fig. 8–Distribution of Shear Stress Extrapolated from 1971 ACI Code

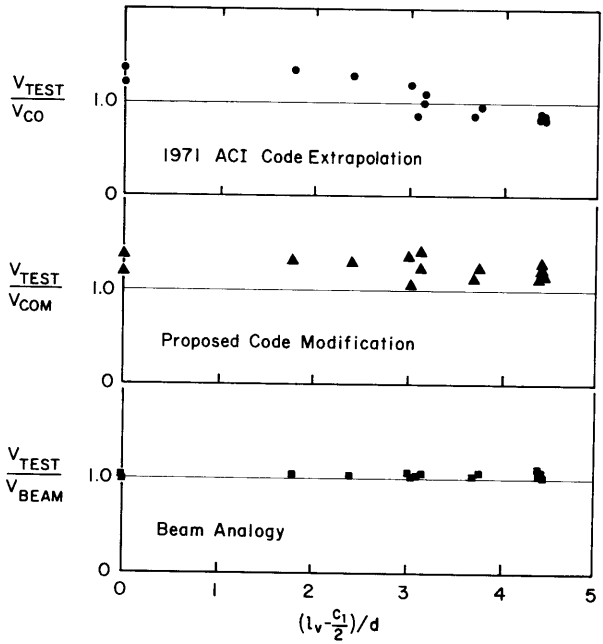

Fig. 9–Comparison of Test Versus Calculated Strengths

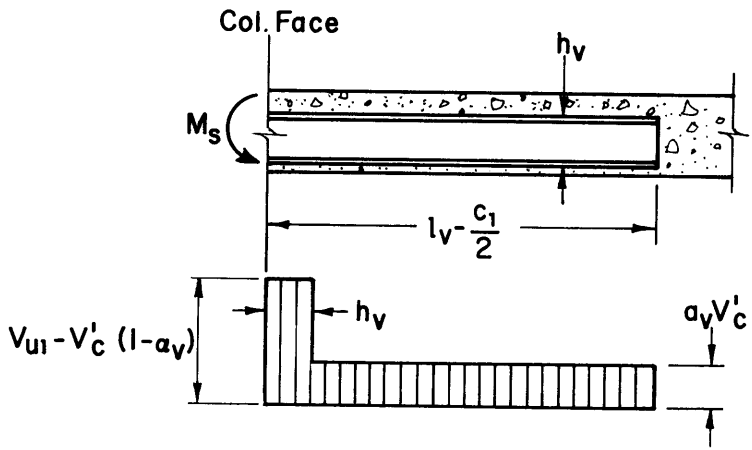

$$M_p \geq M_s = \frac{V_{u1}}{2}\left[h_v+\alpha_v\left(l_v-\frac{c_1}{2}\right)\right] \quad \text{if} \quad V_{u1}=2V'_c$$

Fig. 10–Idealized Shear Distribution at Ultimate Load

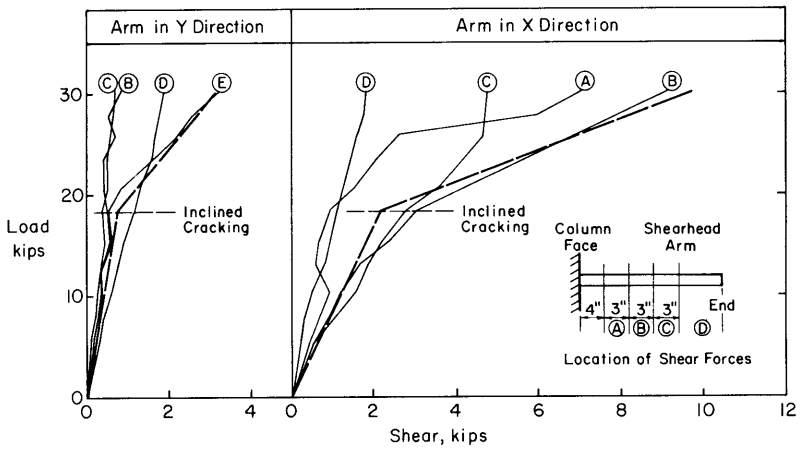

Fig. A1-Load-Shear Relationships for Shearhead of CH4

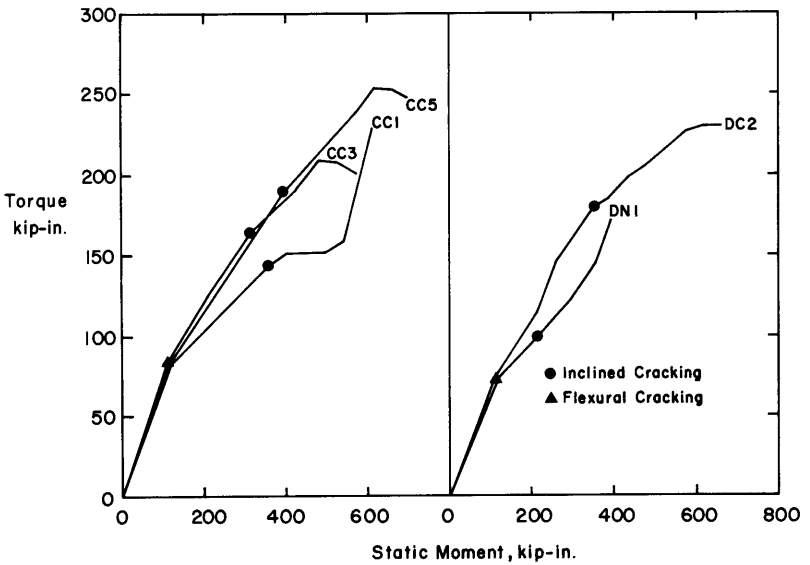

Fig. A2-Comparison of Static Moment and Torque